Cyclic Tests on the Internally Braced RC Frames

H. Ghaffarzadeh and M.R. Maheri

Dept. of Civil Engineering, Shiraz University, Shiraz, Iran, email: maheri@shirazu.ac.ir

ABSTRACT: *Directly-connected internal steel bracing of RC frames has received some attention in recent years, both as a retrofitting measure to increase the shear capacity of the existing RC buildings and as a shear resisting element in the seismic design of new buildings. Although its successful use to upgrade the lateral load capacity of existing Reinforced Concrete (RC) frames has been the subject of a number of studies, guidelines for its use in newly constructed RC frames need to be further developed. An important consideration in the design of steel-braced RC frames is the level of interaction between the strength capacities of the RC frame and the bracing system. In this paper, results of experimental investigations aimed at evaluating the seismic response of brace-frame system and the level of interaction between the bracing system and the RC frame are discussed. For these investigations, cyclic loading tests are conducted on scaled moment resisting frames with and without bracing. Test results confirm the ability of the bracing system to enhance the strength capacity of the RC frame while maintaining adequate ductility. They also provide an insight into the causes and the levels of interaction between the strength capacities of the bracing system and the RC frame.*

Keywords: Steel bracing; Reinforced concrete; Braced RC frames; Cyclic load testing

1. Introduction

Steel bracing is commonly used to increase the seismic shear resistance of steel framed buildings. Recently, the use of steel bracing to upgrade the seismic capacity of existing *RC* frames has also been the subject of several research investigations. Two bracing systems are typically considered, external bracing and internal bracing. In the external bracing system, existing buildings are retrofitted by attaching a local or global steel bracing system to the exterior frames. Architectural concerns and difficulties in providing appropriate connections between the steel bracing and *RC* frames are two of the shortcomings of this method.

In the internal bracing method, the buildings are retrofitted by incorporating a bracing system inside the individual bays of the *RC* frames. The bracing may be attached to the *RC* frame either indirectly or directly. In the indirect internal bracing, a braced steel frame is positioned inside the *RC* frame. As a result, the transfer of load between the steel bracing and the concrete frame is achieved indirectly through the steel frame. The indirect internal bracing method can be costly and technical difficulties in fixing the steel frame to the *RC* frame can be inhibiting. Another shortcoming of this method is that the retrofitted frame is susceptible to the dynamic interaction between the adjoining steel frame and the concrete frame during earthquake loading.

In using the steel bracing for *RC* frames, the earlier investigators focused on the retrofitting aspect of the bracing. They studied external bracing of buildings [1-2] and frames [3] as well as internal indirect bracing of the *RC* frames to seismically retrofit *RC* buildings [4-7]. In recent years, the direct bracing of *RC* frames has attracted more attention since it is less costly and can be adopted not only for retrofitting purposes but also as a viable alternative to *RC* shear walls at pre-construction design level. Maheri and Sahebi [8] first recommended the use of directly connected internal braces

over the use of indirect internal bracing system. In an experimental work, they showed the ability of the bracing system to enhance the strength capacity of the *RC* frame. Later, Tasnimi and Masoomi [9] carried out tests on a number of steel braced *RC* frames and presented some connection types for the brace-frame system. In continuation of previous works, Maheri et al conducted experimental investigations on pushover response of scaled *RC* frames braced with both diagonal bracing and knee bracing systems [10]. In this study the effectiveness of both bracing systems in increasing some seismic performance parameters include the strength and toughness whilst maintaining an adequate ductility was shown. Also, in a theoretical study, Maheri and Akbari presented the behaviour factor, *R*, for this class of dual systems [11].

Connections between the bracing members and the *RC* frame are important to achieve the required lateral load capacity. A number of connections capable of transferring loads to the additional lateral load resisting elements are proposed by several researchers [8, 9, 12]. These connections rely on the use of adhesives, grout, or mechanical anchors. Maheri and Hadjipour [13] proposed a connection that minimizes the eccentricity of the brace member force. This allowed transferring the brace force to the corner of the *RC* frame without producing local damage in concrete members. Using the results of an experimental program conducted on a number of full-scale connections, they also presented design guidelines for the brace-frame connections in new construction.

In this study, the use of directly-connected concentric internal steel bracing for new construction is investigated both experimentally and numerically. In the experimental program, cyclic loading tests were conducted on three scaled frames representing one *RC* moment frame with moderate ductility and two braced *RC* frames. Current seismic codes were used to design the moment frame. For the braced frames, a rational design methodology was adopted using the uncoupled strength capacities of the moment frame and the bracing system. Their test results were compared and discussed. This allowed gaining an improved understanding of the performance of the braced frames and evaluating the adopted design methodology.

2. Experimental Setup

A three-bayed, four-storey frame of a residential building was considered for this study. The building was assumed to be located in a highly seismic area. Two lateral load resisting systems, namely; an *RC* moment frame and a braced *RC* frame, were considered for the selected frame. A mid-span panel, measuring 4.0*m* by 3.0*m*, was isolated from the third floor of each of the load resisting systems, see Figure (1). In this experimental study, only the gravity and earthquake forces induced from analytical results are transferred to the isolated panel. Other effects such as constraint for joint rotation and stiffness interactions are not included in the experimental model. The gravity and earthquake forces acting on these panels were determined in accordance with the Iranian seismic code [14] using the seismic force reduction factor for moment frames with moderate ductility.

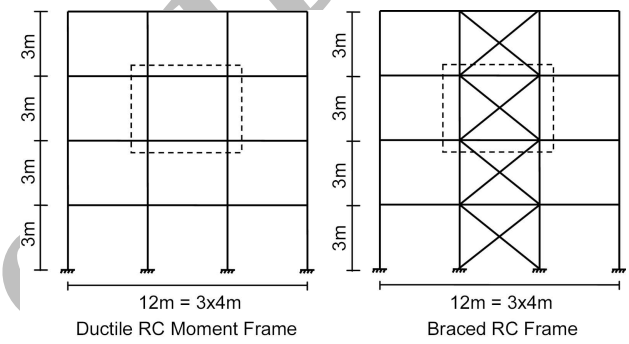

Figure 1. Lateral load resisting system.

The two selected unit frames (panels) from the third floor of the building frames were assumed to be supported by two hinged supports located at the ends of their lower beams. To model the distribution of the bending moments in the actual *RC* frame, the unit frames have to be subjected to two concentrated vertical loads acting on the columns and a concentrated lateral load acting at the level of the upper beam. The gravity and lateral loads acting on these units were calculated using a linear elastic analysis.

The size of the test specimens was determined based on the available laboratory space and the equipment limits. *A* 2/5 scaled model, measuring 1.76*m* by 1.36*m*, was found to be satisfactory. The forces acting on the panels were also scaled down by a factor of (2/5)2. This factor was chosen to keep the stresses in the scaled model similar to those of the full-scale panel. This resulted in a lateral load of 22*kN* and two vertical loads of 35*kN* for the moment frame and the same lateral load of 22*kN* and two vertical loads of 38.5*kN* for the braced frames. Figure (2) shows the unit frames with the assumed design loads.

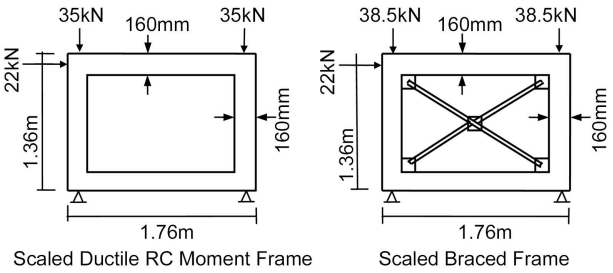

Figure 2. The loading considered for the two model systems.

One moment resisting *RC* frame model, namely *F*1 and two braced *RC* frame models, namely *FX*1 and *FX*2, were designed using the above gravity and lateral loads. The moment frame was designed according to *ACI* 318-02 [15] and its detailing was done in accordance with the *ACI* special provisions for seismic design. Reinforcement details for this frame are shown, on the left hand side, in Figure (3). The beams and columns of the braced frames were designed according to the current standards for the design of RC elements. Detailing was done according to the general detailing requirements. The brace members and their connections were designed according to the current standards for the design of steel elements. AISC-LRFD [16] was used to design the brace members and their welded connections to the guest plates. Their design was also checked using the *AISC* seismic provisions for steel structures [17]. Reinforcement details for the braced frames are also shown on the right hand side of Figure (3).

For the braced *RC* frames, two, 150 x 150 x 8*mm*, steel plates were placed at each of the four inner corners of the *RC* frames prior to casting the specimens. Each plate was anchored to the *RC* frame using four-5/8 inch headed studs as shown in Figure (3). Self-consolidated concrete with 28 days compressive strength of 55 *MPa* was used to cast the frames. The yield strength of the steel reinforcement was also measured as 400*MPa*. Bracing members were then installed by welding their gusset plates to the previously anchored steel plates. A double-angle brace cross-section, consisting of two 25×25×3.2*mm* angles, giving a cross-sectional area of 300mm^2, was chosen for the frame *FX*1 and a *C* 30×3.5*mm* channel with a cross-sectional area of around 500 mm^2 was selected for the frame *FX*2, see Figure (3). The brace members had yield capacities of 300*MPa*. The difference in the brace member cross-section, therefore, made the *FX*2 frame somewhat stronger than the *FX*1 frame.

The model frames were tested using the setup shown in Figure (4). They were subjected to gravity loads using two hydraulic jacks. A special

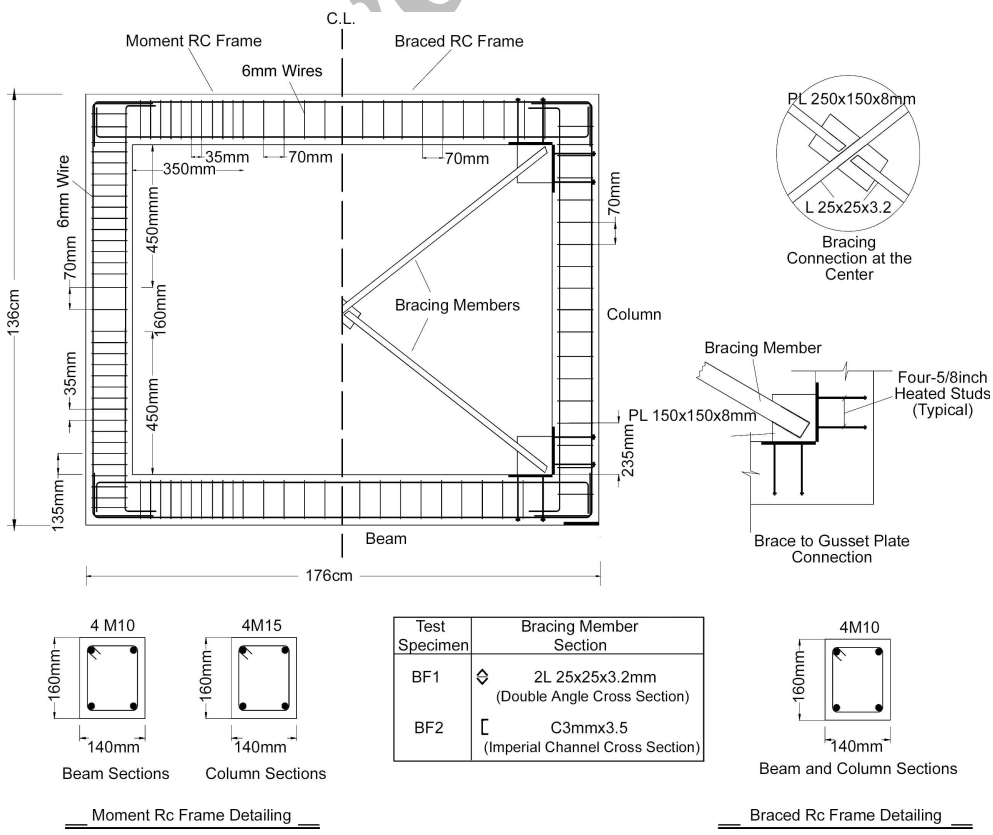

Figure 3. Detailing of the moment RC frame (*F*1) and the braced RC frames (*FX*1 and *FX*2).

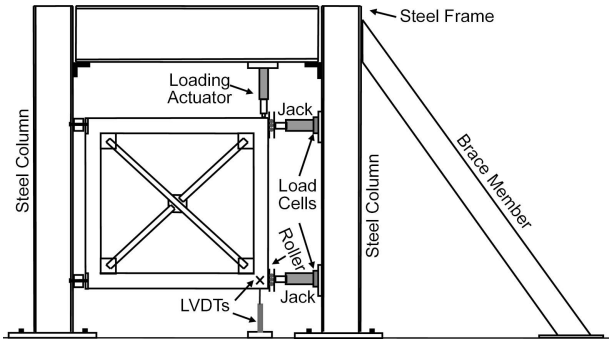

Figure 4. Schematic of the test setup and measurement instrumentations.

roller was developed to allow these jacks to slide on the concrete surface while testing. An actuator with a capacity of 245*kN* and a maximum stroke of 150*mm* was used to apply several cycles of loads using a displacement-controlled approach. In each cycle, the actuator was first pulled to a displacement, *d*1, of 5*mm*, then pushed to the same displacement. The value of d1 was increased in the following cycles by an increment of 5*mm*.

The behaviour of the test models was monitored by using electrical and mechanical instrumentations including: Load cells were attached to the hydraulic jacks and the actuator to measure applied loads, Linear Voltage Differential Transformers (*LVDTs*) to measure the lateral deformations, and electronic strain gauges to monitor local strains in the reinforcement bars as well as steel bracing elements. One *LDVT* was used to measure the lateral drift and two others, placed diagonally over each other, were used to measure the internal displacements at the corner of the *RC* frame. The locations of test instrumentation are illustrated in Figure (4). The data were recorded at intervals of one second. A discussion of the test results is given below.

3. Experimental Observations and Results

3.1. Hysteretic Response and Load Capacity

Figure (5) shows a photograph of the moment frame after the completion of the test. Figure (6) also shows details of crack pattern in frame. The hysteretic lateral load-drift curves for this frame are also shown in Figure (7). At a load of 37.5 *kN*, yielding of the lower bars of the lower beam initiated the plastic response. Failure occurred by plastic hinging at the ends of the upper and lower beams at a load of 55*kN*. The drifts of the moment frame at the yield load and the maximum load were measured as 1.5% and 4.6%, respectively. The relationship between the

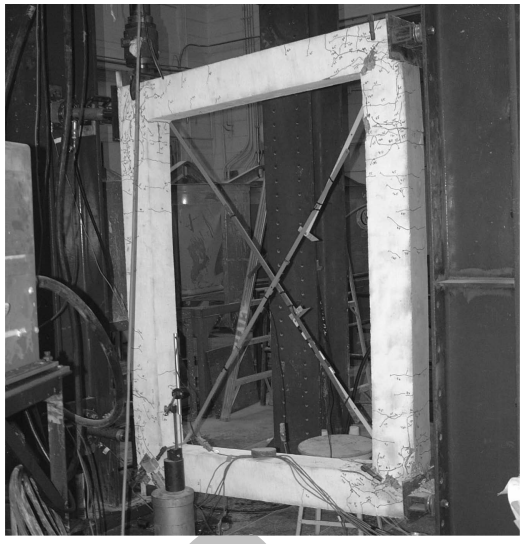

Figure 5. Photo of the moment frame, *F*1, after the test.

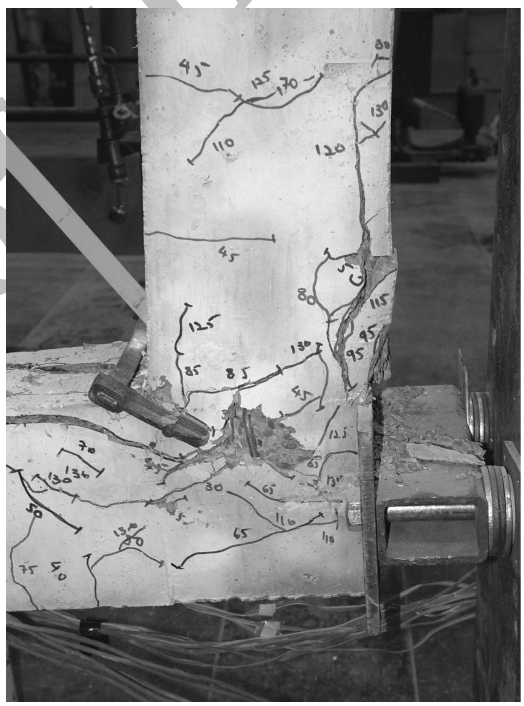

Figure 6. Pattern of cracking in the moment frame *F*1.

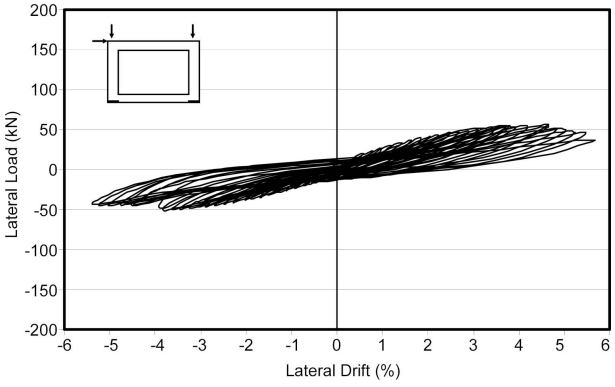

Figure 7. Lateral load-drift hysteresis of frame *F*1.

lateral load and diagonal displacement of the *RC* frame is also shown in Figure (8).

The cyclic lateral force-drift relationship for frame *FX*1 is shown in Figure (9). At a drift of 1.9%, corresponding to a lateral load of 105*kN*, yielding of the double-angle bracing member initiated the plastic response. A significant drop in the lateral load capacity was observed at a load of 140*kN* (drift of 4.0%). This was noted to be due to the buckling of brace members. Following this, the lateral load capacity was mainly provided by the *RC* frame, which failed when plastic hinges were formed at the ends of the lower and upper beams, see Figure (10). As the lateral load capacity reduced, at a load of about 105*kN*, the reinforcement in the *RC* frame reached the yield strain, see Figure (9). The diagonal displacement variation of the *FX*1 frame versus the lateral load is also plotted in Figure (11).

Figure (12) shows the lateral force-drift relationship for frame *FX*2. The measured strain of the longitudinal beam reinforcement during the test showed that the yielding occurred at a load of about 140*kN*. The lateral capacity of the frame was not however affected because the bracing members were still acting in the elastic range. Testing was continued to a load of 200*kN*, which was the loading capacity of the actuator and subsequently the test was terminated. The diagonal displacement variation of the specimen *FX*2 versus the lateral load is also plotted in Figure (13). It is evident in this figure that the response of the frame to the cyclic loading was

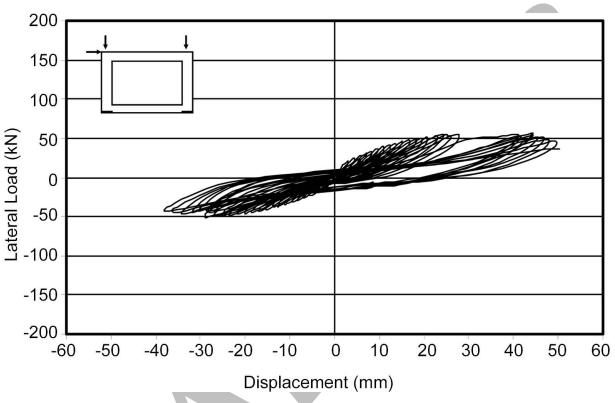

Figure 8. Lateral load versus diagonal displacement hysteresis of frame *F*1.

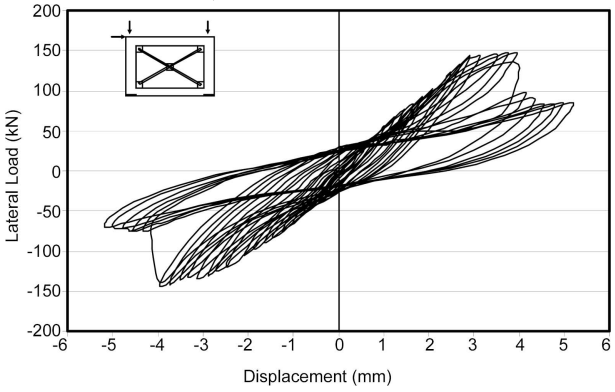

Figure 9. Lateral load-drift hysteresis of frame *FX*1.

Figure 10. Photo of the braced frame, *FX*1, after the test.

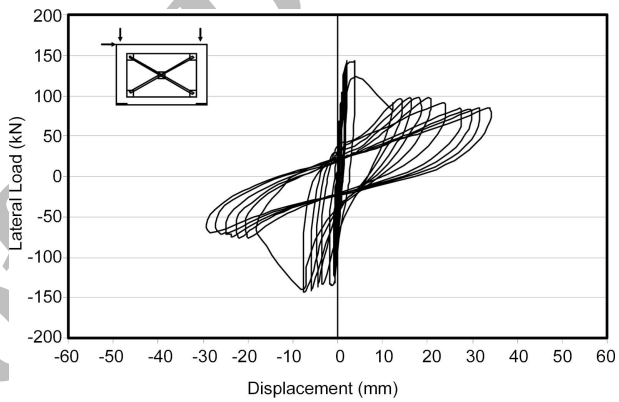

Figure 11. Lateral load versus diagonal displacement hysteresis of frame *FX*1.

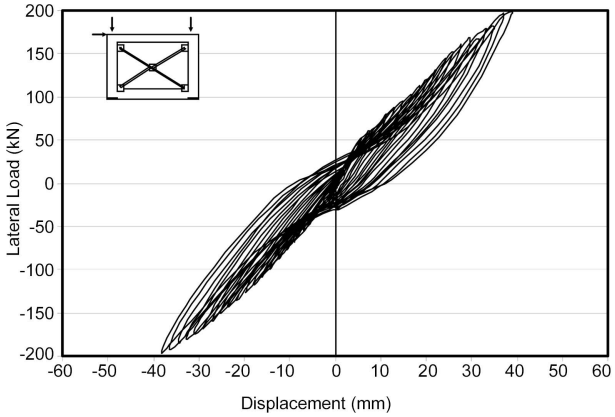

Figure 12. Lateral load-drift hysteresis of frame *FX*2.

almost linear on the diagonal. A summary of the yield loads and the maximum sustainable loads and their corresponding displacement ratios for the three tested frames are presented in Table (1).

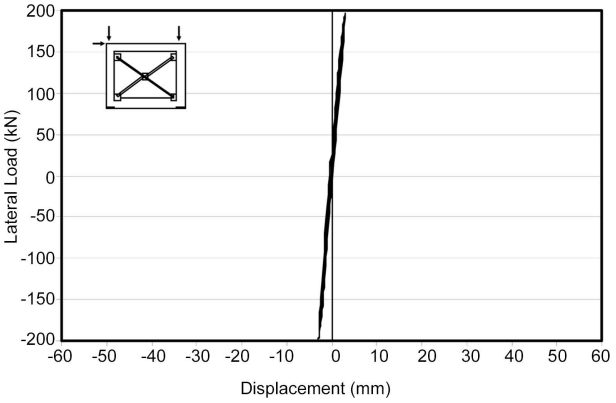

Figure 13. Lateral load versus diagonal displacement hysteresis of frame *FX*2.

Table 1. The yield and ultimate strength capacities and their corresponding relative displacements.

Frame	Yield Strength (kN)	Yield Displacement (%)	Ultimate Strength (kN)	Displacement at Ultimate Strength (%)
F1	37.5	1.5	55	4.6
FX1	105	1.9	140	4.0
FX2	140	2.8	200	3.9

3.2. Stiffness Degradation

The lateral stiffness was evaluated as the peak-to-peak stiffness of the frame load-displacement relationship. It was calculated as the slope of the line joining the peak of positive and negative loads at a given cycle. The lateral stiffness is an index of the response of the frame from one cycle to the following cycle. Figure (14) illustrates a plot of the lateral stiffness for the three tested frames. Before buckling of the compressive brace, the diagram shows that the lateral stiffness of the frame *FX*1 was more than double that of the frame *F*1 and that the rate of stiffness degradation for both systems was almost equal. However, after buckling of the compressive brace, the lateral stiffness of the frame *FX*1 dropped and became comparable to that of the moment frame, see Figure (14). Also, the *FX*2 frame, having more robust bracing members compared to the frame *FX*1, shows higher hysteretic stiffness compared to the latter. However, both frames show a similar rate of stiffness degradation.

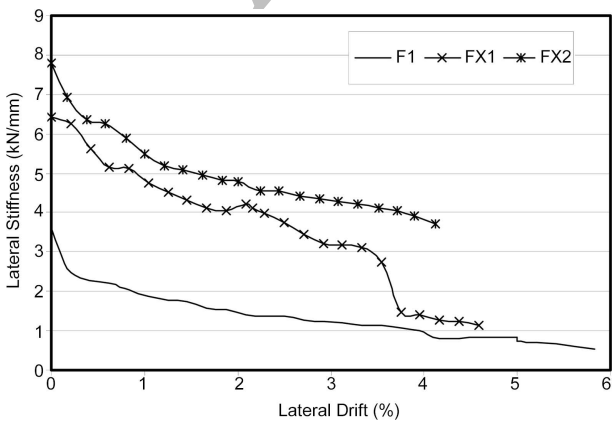

Figure 14. Degradation of the lateral stiffness of test frames.

3.3. Energy Dissipation Capacity (Toughness)

The ability of a structure to dissipate the seismic induced energy is an accurate measure for its expected seismic performance. In this study, the energy dissipated by the three tested frames during the cyclic load testing was calculated as the area enclosed by each hysteretic loop. Figure (15) shows a plot of the energy dissipated during a load cycle versus the lateral drift. Also the energy dissipated by each test frame after a number of selected cycles is presented in Table (2). It is observed that at low drift levels, the energy dissipated by the frames *FX*1 and *FX*2 was comparable with that of the frame *F*1. At higher levels of drift, it is clear that the energy dissipated by the braced frames is much higher than that by the moment frame. This proves that the overall seismic performance of the braced frames is expected to be superior to that of the moment frame.

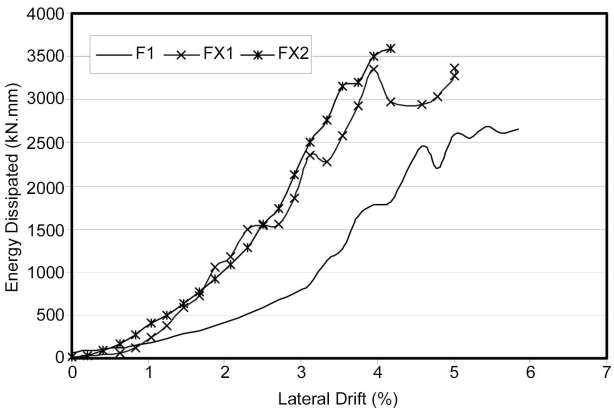

Figure 15. Variation of energy dissipation with the applied displacement.

Table 2. Energy dissipation capacity of the test frames.

Frame	Cumulative energy dissipated (kN.mm)				
	Cycle 5	Cycle 10	Cycle 15	Cycle 20	Cycle 25
F1	600	2229	5619	13256	25474
FX1	451	4367	13163	27276	32875
FX2	570	3807	11540	26714	-

3.4. Ductility

Ductility is another important factor when considering the seismic response of structures. In this study, ductility is measured both as the ratio of the displacement pertaining to the maximum force Δ_{max}, to the displacement at yield Δ_y and as the ratio of the maximum displacement $\Delta_{available}$ to the displacement at yield point Δ_y of the model frames. These are calculated and shown in Table (3). As it was expected, the addition of x-bracing system somewhat reduces the ductility of a ductile frame, but the reduction in ductility does not affect the energy dissipation capacity of the frames. Maheri et al [10] showed in an earlier study that if, sustaining a particular ductility level is of prime importance, instead of the common *X*-bracing, alternative bracing systems, such as knee-bracing, could be adopted.

3.5. Capacity Interaction between the Bracing System and Moment Frame

An important consideration in the design of steel braced *RC* frames is the level of possible interaction between the strength capacities of the *RC* frame and the bracing system. To investigate this, the corresponding forces in the bracing systems alone were evaluated by considering the relevant test displacements on the diagonals.

A simple bilinear model for steel which accounts for cyclic effects was assumed and used to represent the force-deflection envelop curve of steel bracing system alone. The envelop curve of the calculated force-drift relationship for the *FX*1 bracing system alone (marked as No. 2 in the figure) is plotted in Figure (16). Also plotted in this figure, for comparison, are the experimental envelop of the force-drift relationship of the moment frame alone, *F*1 (marked as No. 1 in the figure) and the experimental envelop of the force-drift relationship of the *FX*1 braced frame. To be able to gain an insight into the level of capacity interaction between different elements, the envelop curves of the bracing system alone (2) and the moment *RC* frame (1) are added together to obtain the sum

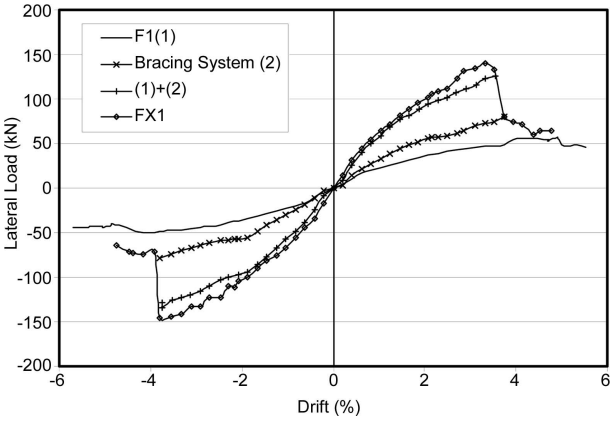

Figure 16. Comparison between the experimental lateral load-drift envelop curves of the moment frame, *F*1, bracing system and the braced RC frame, *FX*1.

strength capacity of the two elements as also presented in Figure (16) ((1)+(2)). By comparing the sum strength capacity of the two constituent elements with the actual strength capacity of the braced frame, it is evident that the actual braced frame exhibits a larger capacity than the sum of the capacities of the two elements. This means that by adding a bracing system to an *RC* frame, the strength capacity of the *RC* frame is increased beyond the capacity of the bracing system. The positive interaction is evidently due to the stiffening effects of the connections between the *RC* frame and the bracing system. The capacity interaction for the frame *FX*1 is measured, as the minimum of all the evaluated values, at 8.5 percent. It should be noted that although the transverse reinforcements in the moment frame *F*1 and the braced frames *FX*1 and *FX*2 are different, see Figure (3); their longitudinal reinforcements are the same, rendering similar flexural capacities for the two *RC* frames, as was also noted in the test results. This enables us to make a viable capacity interaction comparison as discussed above.

Similarly, the calculated strength capacity of the bracing system of frame *FX*2 and the experimental strength capacities of the moment frame, *F*1, and the braced frame *FX*2 are plotted in Figure (17). Also plotted in this figure is the sum of the strength

Table 3. The ductility of the test frames.

Frame	Yield Displacement (D_y) (*mm*)	Displacement at Ultimate Strength (D_{max})(*mm*)	Maximum Available Displacement ($D_{available}$)(*mm*)	Ductility Corresponding to D_{max}	Ductility Corresponding to $D_{available}$
*F*1	18.0	55.4	68.0	3.1	3.8
*FX*1	22.5	47.5	62.5	2.1	2.8
*FX*2	33.0	45.6	-	1.4	-

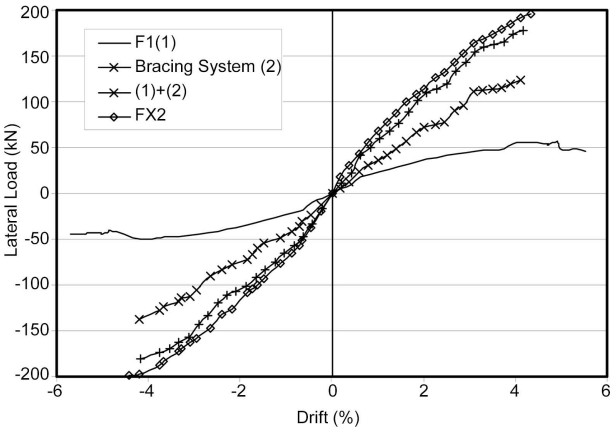

Figure 17. Comparison between the experimental lateral load-drift envelop curves of the moment frame, *F*1, bracing system and the braced RC frame, *FX*2.

capacities of the bracing system and the *RC* frame alone. Similar added increases in the strength can be seen in this case. The capacity interaction for the frame *FX*2 is measured at 7.0 percent.

4. Non-Linear Pushover Analysis of the Model Frames

To further investigate the level of capacity interaction between the steel bracing and *RC* frame, non-linear pushover numerical analyses of the moment frame, braced frames and the bracing systems were carried out. The OpenSEES (Open System for Earthquake Engineering Simulation) program was utilised to numerically model the frames. The beams and columns of the frames were modeled using nonlinear beam-column element of the program. To model the steel bracing members, the truss element was considered. Initially the numerical model was calibrated by comparing the results of the non-linear pushover analysis of the moment frame *F*1 with the envelop curve obtained from the cyclic tests on this frame. The results of the numerical analysis and the experimental response compare well as seen in Figure (18).

Nonlinear pushover analyses of the braced frames, *FX*1 and *FX*2 were then carried out. In the numerical models of the braced frames, the effects of brace-frame connections on reducing the effective lengths of the frame members were considered. In a similar manner to the comparative study presented in the previous section, the sum of the numerical strength capacities of the individual *RC* frame and the bracing system were calculated and compared to the strength capacity of the braced frames. These are shown in Figures (19) and (20) for the frames *FX*1 and *FX*2, respectively. The calculated load capacity increase due to the addition of bracing system is 7.0 percent for frame *FX*1 and 6.8 percent for frame *FX*2. These calculated interaction levels compare well with the previously presented experimental values of 8.5 percent and 7.0 percent, respectively.

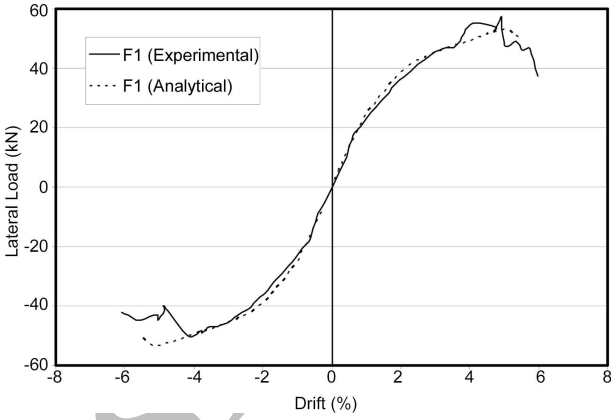

Figure 18. Calibration of the numerical model of moment frame *F*1 with the experimental results.

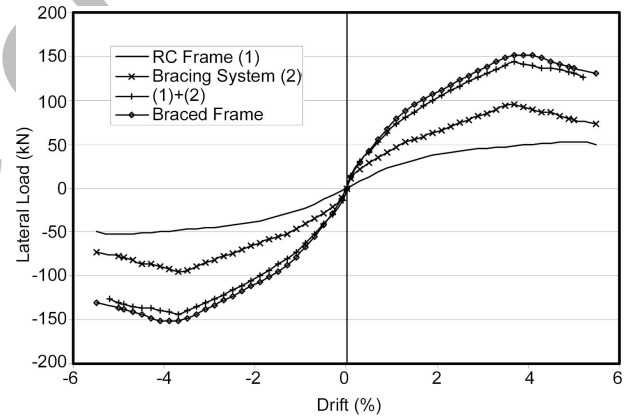

Figure 19. Comparison between the numerical lateral load-drift pushover curves of the moment frame, *F*1, bracing system and the braced RC frame, *FX*1.

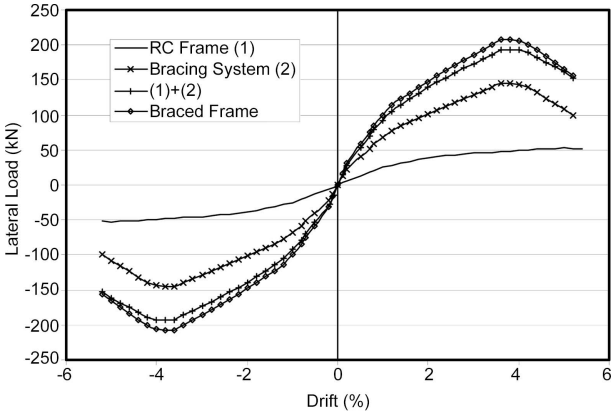

Figure 20. Comparison between the numerical lateral load-drift pushover curves of the moment frame, *F*1, bracing system and the braced RC frame, *FX*2.

5. Conclusions

An experimental investigation was conducted to assess the seismic behaviour of steel braced *RC* frames. Three frames, one conventional moment frame with moderate ductility and two frames braced with diagonal steel bracing were designed using the same seismic force reduction factor. The following conclusions are drawn based on the results of the cyclic tests:

- The desired increase in the load capacity and the reduction in the lateral drift can be easily achieved by incorporating a steel bracing system inside the individual panels of the ductile and non-ductile *RC* frames. The test results indicate that this dual system, exhibits a substantial energy dissipation capacity and an adequate ductility capacity.
- It is shown in this paper that the design of *RC* members in a braced *RC* frame can be carried out using the conventional *RC* design methods. The brace members and their connections can also be designed using a similar procedure to that for braces in steel structures. This simple procedure is however conservative leading to an over-design. To carry out a more representing design, the strength capacity interaction between the bracing system and the *RC* frame should be considered.
- The strength capacity interaction stems mainly from the modifying effects of the brace-frame connections on the stiffness of the dual system. For the 2/5 model frames tested, the capacity interaction levels ranged from 7 percent to 9 percent.
- Further, numerical works are underway to determine the range of capacity interaction for full scale frames of different sizes and configurations so that appropriate guidelines for design of such systems can be presented.

Acknowledgements

The experiments presented in this paper were conducted by the senior author in the laboratories of the Civil Engineering Department of the University of Western Ontario (UWO), Canada. The authors wish to express their gratitude to Drs. Nehdi and Youssef of UWO for their financial and technical help during that period.

References

1. Bush, T.D., Jones E.A., and Jirsa, J.O. (1991). "Behavior of RC Frame Strengthened Using Structural-Steel Bracing", *J. Struct. Eng-ASCE*, **117**(4), 1115-1126.

2. Badoux, M. and Jirsa, J.O. (1990). "Steel Bracing of RC Frames for Seismic Retrofitting", *J. Struct. Eng., ASCE*, **116**(1), 55-74.

3. Nateghi-Alahi, F. (1995). "Seismic Strengthening of Eight-Storey RC Apartment Building Using Steel Braces", *Engineering Structures*, **17**(6), 455-461.

4. Higashi, Y., Endo, T., and Shimizu, Y. (1981). "Experimental Studies on Retrofitting of Reinforced Concrete Structural Members", *Proceedings of the Second Seminar on Repair and Retrofit of Structures*, Ann Arbor, MI, National Science Foundation, 126-155.

5. Rodriguez, M. and Park, R. (1991). "Repair and Strengthening of Reinforced Concrete Buildings for Seismic Resistance", *Earthquake Spectra*, **7**(3), 439-459.

6. Masri, A.C. and Goel, S.C. (1996). "Seismic Design and Testing of an RC Slab-Column Frame Strengthened by Steel Bracing", *Earthquake Spectra*, **12**(4), 645-666.

7. Ohishi, H., Takahashi, M., and Yamazaki, Y. (1988). "A Seismic Strengthening Design and Practice of an Existing Reinforced Concrete School Building in Shizuoka City", *Proceedings of the Ninth World Conference on Earthquake Engineering*, Japan, **VII**, 415-420.

8. Maheri, M.R. and Sahebi, A. (1997). "Use of Steel Bracing in Reinforced Concrete Frames", *Engineering Structures*, **19**(12), 1018-1024.

9. Tasnimi, A.A. and Masoomi, A. (1999). "Evaluation of Response of Reinforced Concrete Frames Strengthened with Steel Bracing", *Proceedings of the Third International Conference on Seismology and Earthquake Engineering*, Iran, (in Farsi).

10. Maheri, M.R., Kousari, R., and Razazan, M., "Pushover Tests on Steel X-Braced and

Knee-Braced RC Frames", *Engineering Structures*, **25**(13), 1697-1705.

11. Maheri, M.R. and Akbari, R. (2003). "Seismic Behaviour Factor, R, for Steel X-Braced and Knee-Braced RC Buildings", *Engineering Structures*, **25**(12), 1505-1513.

12. Canales, M.D., Broseno, de la, and Vega, R. (1992). "Retrofitting Techniques Used in Telephone Buildings in Mexico", *Proceedings of the Tenth World Conference on Earthquake Engineering*, 5143-5147.

13. Maheri, M.R. and Hadjipour, A. (2003). "Experimental Investigation and Design of Steel Brace Connection to RC Frame", *Engineering Structures*, **25**(13), 1707-1714.

14. Iranian Code of Practice for Seismic Resistance Design of Buildings. Standard No. 2800, 2nd Ed.

15. ACI Committee 318. (2002). "Building Code Requirements for Reinforced Concrete (ACI 318-302)", American Concrete Institute, Detroit, MI.

16. AISC (2001). "Manual of Steel Construction: Load and Resistance Factor Design", 3rd Edition, Chicago (IL), American Institute of Steel Construction.

17. AISC (2002). "Seismic Provisions for Structural Steel Buildings", Chicago (IL), American Institute of Steel Construction.